Heliyon 6 (2020) e05486

Contents lists available at ScienceDirect

Heliyon

journal homepage: www.cell.com/heliyon

Research article

Preparation and characterization of cellulose nanocrystal extracted from ramie fibers by sulfuric acid hydrolysis

Kusmono *, R. Faiz Listyanda, Muhammad Waziz Wildan, Mochammad Noer Ilman

Department of Mechanical and Industrial Engineering, Faculty of Engineering, Universitas Gadjah Mada, Jalan Grafika No. 2, Yogyakarta, 55281, Indonesia

ARTICLE INFO

Keywords:
Materials science
Materials chemistry
Biotechnology
Ramie fibers
Cellulose nanocrystal
Sulfuric acid hydrolysis

ABSTRACT

Cellulose nanocrystals (CNCs) were isolated from ramie fibers through chemical pretreatments accompanied by sulfuric acid hydrolysis. The influences of both temperature and hydrolysis time on the properties of CNCs were discussed in the present study. The characterization of CNCs was conducted using FT-IR, XRD, TEM, and TGA. The results showed the characteristics of obtained CNCs were influenced significantly by both temperature and time of hydrolysis. The crystallinity, dimensions, and thermal stability of CNCs were found to reduce by increasing both temperature and reaction time of hydrolysis. The optimal hydrolysis parameters were achieved at 45 °C for 30 min with 58% sulfuric acid to produce CNCs, rod-like particles with a high crystallinity (90.77%), diameter (6.67 nm), length (145.61 nm), and best thermal stability among all CNCs. The obtained CNCs had a higher potential for application of alternative reinforcing fillers in the nanocomposites.

1. Introduction

In recent years, cellulose has attracted great interest owing to its unique characteristics such as abundant availability in nature, renewable, environmentally friendly, biocompatibility, and cost-effective reinforcement of composites [1]. Cellulose can be obtained from large types of plants, animals, and some bacteria that becoming the most abundant biopolymer on earth [2]. Cellulose nanocrystals (CNCs) are high crystalline, defect-free, needle-like particles with an average diameter of 5–10 nm and an average length of around 100 nm prepared with the elimination of amorphous parts in cellulose fibers via acid hydrolysis [3, 4]. CNC is a cellulose-based material that promises to be due to its attractive properties including nanometer size, low toxicity, biocompatibility, biodegradability, excellent mechanical, and optical properties [4, 5]. Owing to its attractive characteristics, CNC has been proven to be extensively used in a lot of applications including optical apparatuses, regenerative medicine, and as a reinforcement material of nanocomposites [6].

CNCs can be isolated from various agro-industrial wastes. In the literature, CNCs have been prepared from many different resources such as wheat straw [7], sisal [8], pineapple leaves [9], coconut husk fibers [10], banana [11], sugarcane bagasse [12], bamboo [13], mengkuang leaves [14], rice straw [15], cotton linter [16], kenaf bast [17], corn husk [18], Acacia mangium [19], oil palm fronds [20], doum leaves [21], cassava bagasse [22], sugar palm fibers [23], apple pomace [3], cotton pulp [24] and date palm [25]. Ramie fiber is a potential source of cellulose to produce CNC due to its high cellulose (72.68%), hemicellulose (13.70%), and very low contents of lignin (0.38%) [26]. In this work, the ramie fiber was chosen as a source of cellulose owing to high cellulose content and low non-cellulose substances. CNCs prepared from ramie fibers have been reported in several literatures. Habibi et al. [27] produced CNC from ramie fibers via sulfuric acid hydrolysis (65% (w/w) H_2SO_4 solution) and combined it with poly (3-caprolactone) (PCL) matrix to make PCL/CNC bio-nanocomposite films. They found that both elastic and storage modulus of PCL increased significantly by the presence of CNC. In addition, Habibi et al. [28] prepared CNCs from three different natural fibers such as cotton, sisal, and ramie fibers through sulfuric acid hydrolysis. In addition, cellulose surfaces model based on CNCs were produced with the Langmuir-Schaeffer method. They concluded that the Langmuir-Schaeffer (LS) horizontal deposition method was obtained appropriate for preparing stable, strong monolayers of CNCs from sisal, cotton, and ramie. Recently, cellulose nanofibers produced from ramie fibers by a combined chemical-ultrasonic method were demonstrated by Syafri et al. [29]. They obtained the cellulose nanofibers with 9.9–89.1 nm in diameter and 1 μm in length, respectively. Although the producing CNCs from ramie fiber has been made by previous researchers, studies on the influence of hydrolysis parameters on the characteristics of the gained CNCs have not yet been reported.

* Corresponding author.
E-mail address: kusmono@ugm.ac.id (Kusmono).

https://doi.org/10.1016/j.heliyon.2020.e05486
Received 7 March 2020; Received in revised form 28 May 2020; Accepted 6 November 2020

Several methods for producing nanocelluloses including cellulose nanocrystals (CNCs), cellulose nanofibers (CNFs), and bacterial nanocelluloses (BNCs) have been used by numerous researchers [2] such as the mechanical method [30, 31], TEMPO oxidative method [32], ionic liquid method [33], enzymatic method [34], combination method (oxidative or enzymatic and mechanical) [35, 36, 37], sulfuric acid hydrolysis [13, 14, 15], hydrochloric acid hydrolysis [38, 39], phosphoric acid hydrolysis [40, 41], formic acid hydrolysis [42], combined sulfuric acid/oxalic acid hydrolysis [43], mixed sulfuric acid/acetic acid hydrolysis [44], $FeCl_3$-catalyzed deep eutectic solvent system (DES) treatment [45], and mixed chemical-ultrasonic treatments [29]. Among all these methods, sulfuric acid hydrolysis has been recognized as the method most widely used for preparing CNCs because the process is simple and results in nanoparticle (100–1000 nm) with highly crystalline and stiff. The extraction of CNC commonly consists of two processes, namely chemical purification and acid hydrolysis [46]. The chemical purification was carried out to eliminate non-cellulose contents (wax, lignin, and hemicellulose) and produce chemically purified cellulose (CPC). The chemical purification process composes several steps including dewaxing, bleaching, and alkali treatments [47]. The acid hydrolysis was performed to the CPC to remove amorphous domains. Sulfuric acid hydrolysis has become the most extensively used method to isolate CNCs because it has been proven effective in the elimination of amorphous components and resulting in stable CNC suspensions [48]. The characteristics of gained CNCs are strongly influenced by several parameters including type and concentration of acid, temperature, time, and acid to pulp ratio.

In this study, CNCs were prepared from ramie fibers by chemical purification accompanied by sulfuric acid hydrolysis. The chemical purification process was performed via de-waxing using toluene and ethanol solution, bleaching using acidified sodium chlorite, and alkali treatments. The purified fibers were then hydrolyzed using sulfuric acid at different conditions. The influences of hydrolysis conditions (temperature and hydrolysis time) on the properties of obtained CNCs were evaluated by FT-IR, XRD, TEM, and TGA.

2. Experimental

2.1. Materials

Dried ramie fibers (Boehmeria nivea) were provided by Balai Penelitian Tanaman Pemanis dan Serat (Balittas) Malang, East Java, Indonesia. In our previous results [26], the ramie fibers contained α-cellulose (72.68%), hemicellulose (13.70%), lignin (0.38%), and others (13.24%). Sulfuric acid with a 96.1% concentration was supplied from Mallinckrodt, Ireland. Toluene (99.9%), sodium chlorite ($NaClO_2$), acetic acid (100%), and sodium hydroxide (99%) were bought from Merck, USA. Ethanol (99.5%) was bought from Sigma-Aldrich, USA.

2.2. Purification of cellulose

Chemically purified cellulose (CPC) was prepared by application of several chemical pretreatments on the ramie fibers. The amorphous components of the ramie fibers were released via some chemical pretreatments (de-waxing, bleaching, and alkalization) to find chemically purified cellulose (CPC). Initially, the dried ramie fibers were cut to a length of about 1 cm, ground, and then sieved into 30 mesh. The ramie fibers were de-waxed in a Soxhlet equipment with a 2:1 (v/v) mixture of toluene and ethanol for 20 cycles. After that, the solvent and impurities were eliminated by washing in 96 wt% alcohol and the fibers were heated at 80 °C for 2 h. The de-waxed fibers were bleached using 0.7% (w/v) ($NaClO_2$ solution with the incorporation of acetic acid solution with a ratio of fiber to acid of 1:50 gr/ml until the pH of 4. This mixture was stirred using the magnetic stirrer at 70 °C for 1 h and rinsed with the distilled water until it achieved the neutral pH. The fibers were then treated by alkali using a 2% (w/v) NaOH solution with a ratio of fiber to alkali of 1:50 g/ml. The fiber suspension was stirred at 90 °C for 2 h with magnetic stirrer. The fibers were rinsed with the distilled water, dried at 80 °C for 3 h, and finally produced CPC. The illustration of the purification process can be presented in Figure 1.

2.3. Extraction of nanocrystalline cellulose

CNCs were produced by sulfuric acid hydrolysis of obtained CPC. Two hydrolysis parameters (temperature and hydrolysis time) were investigated at a constant concentration of 58 wt% and CPC to acid ratio of 1:20 under magnetic stirring. Based on our previous studies [49], the optimal H_2SO_4 concentration was achieved at 58% with the highest crystallinity index of 90.77%. The influences of temperatures (45, 55, 65 °C) and reaction times (30, 45, 60 min) of hydrolysis on the properties of CNCs were studied with a constant sulfuric acid concentration (58 wt%). The hydrolysis was conducted using a sulfuric acid solution (58% (w/w), 1:20 g/ml (CPC: dilute sulfuric acid) under different temperatures of 45, 55, and 65 °C at a constant time of 30 min. Other hydrolyzes were performed at various hydrolysis times of 30, 45, and 60 min at a constant temperature of 45 °C and 58% sulfuric acid concentration. Furthermore, the suspension was cooled into cold distilled water (about 5 °C) by a ratio of suspension to the cold water of 1:20 (v/v) to stop hydrolysis. Centrifugation was conducted at 4000 rpm for 15 min to abolish the acid solution. CNC precipitates were collected and rinsed with distilled water to neutral condition. The ultra-sonication of CNCs suspension was then performed for 1 min by a 50% amplitude to obtain the uniform CNC suspensions. Partly CNCs were accumulated for the TEM observation and others were freeze-dried for FT-IR, XRD, and TGA analysis. The schematic representation of CNCs isolation was displayed in Figure 2.

2.4. Characterization

2.4.1. Fourier transform infrared (FT-IR) spectroscopy

Changes in chemical structures of the samples after the purification and hydrolysis processes were investigated by FT-IR spectra. FT-IR spectra were analyzed on an infrared spectrophotometer (IRPrestige21 machine from Shimadzu) at wavenumbers ranging from 400-4000 cm^{-1}.

2.4.2. X-ray diffraction (XRD)

The diffraction patterns of untreated ramie fiber, CPC, and CNCs were measured in the range 2θ = 10–40° with Emperyan (Malvern PANalytical) x-ray diffractometer using Ni-filtered Cu Kα radiation (λ = 1.5406 Å) at 40 kV and 30 mA. The crystallinity index and crystallite size were analyzed using the diffraction pattern. The crystallinity index was computed according to the Segal empirical method [50] as in Eq. (1):

$$CrI = \frac{(I_{200} - I_{am})}{I_{200}} \times 100\% \quad (1)$$

where, $I_{200}$is the intensity of crystallites peak at approximately 2θ = 22.5° and I_{am} is the intensity of the amorphous cellulose at 2θ = 18–19°. The crystallite size (t) was calculated by the Scherrer equation [51] as in Eq. (2) below:

$$t = \frac{K\lambda}{\beta_{1/2}\cos\theta} \quad (2)$$

where K (0.91) is the Scherrer constant, λ (1.54060 Å) is the radiation wavelength, $\beta_{1/2}$ is the full width at the half maximum (FWHM) of (200) diffraction peak in radians, and θ is the corresponding Bragg's angle.

2.4.3. Transmission electron microscopy (TEM)

The structure and dimensions of CNCs were characterized using the TEM (JEOL type JEM-1400 Electron Microscope, Japan) at of 120–200 kV. A drop (10 μL) of CNC suspension was placed on the copper grids covered by a carbon layer for examination. The diameter and length of

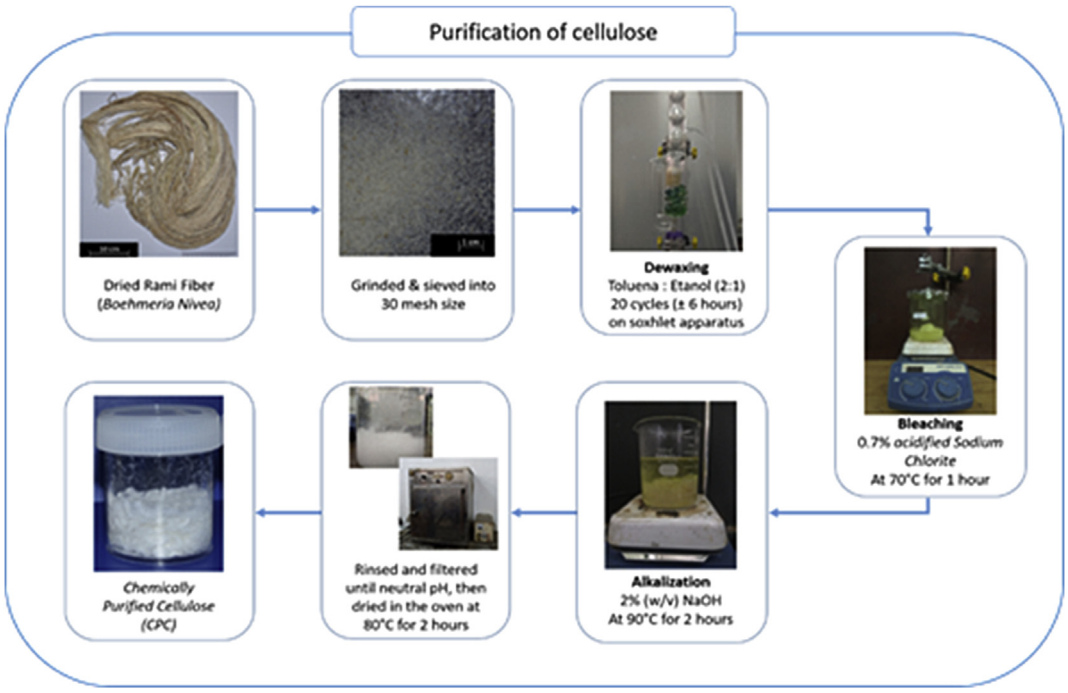

Figure 1. Cellulose purification process of ramie fibers.

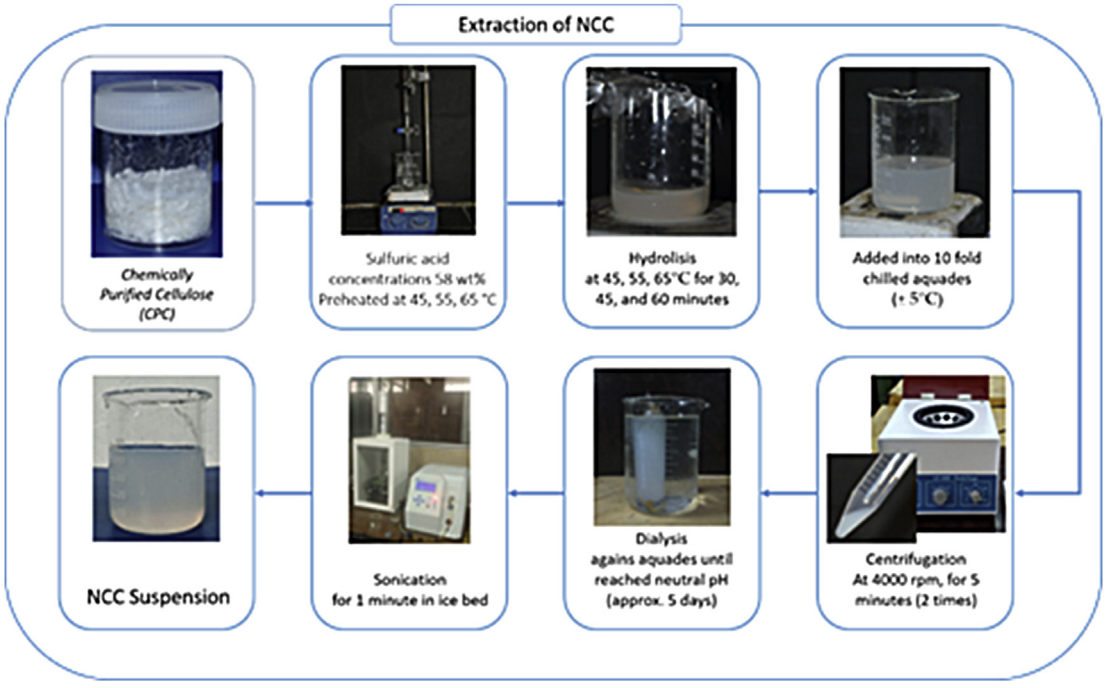

Figure 2. Isolation process of cellulose nanocrystals.

the CNC particles were determined with ImageJ software from the TEM images.

2.4.4. Thermogravimetric analysis (TGA)

The thermal properties were analyzed by TGA (LINSEIS machine Type TA PT 1600) in the temperature range of 30–600 °C in the same heating rate of 10°/min at a flow rate of 4 L/h under the nitrogen atmosphere.

3. Results and discussion

3.1. Fourier transform infrared (FT-IR) spectroscopy

Figure 3 shows the FT-IR spectra of untreated ramie fibers, CPC, and gained CNCs with variations in temperature and duration of hydrolysis. All samples showed almost the same spectra showing no changes in their chemical composition during the purification and hydrolysis of sulfuric

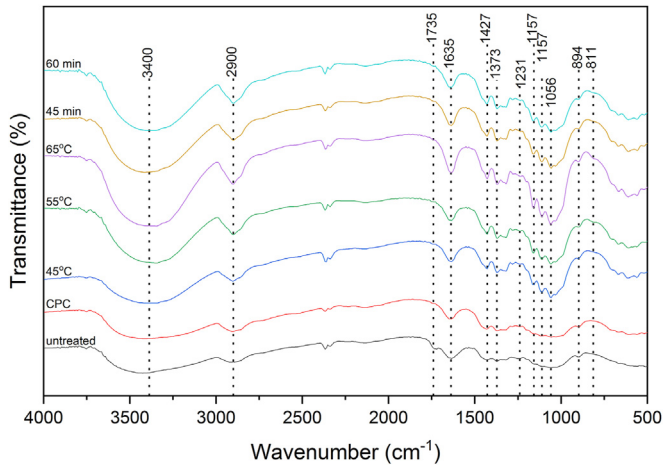

Figure 3. FTIR spectra of untreated ramie fibers, CPC, and CNCs at various hydrolysis temperatures and durations.

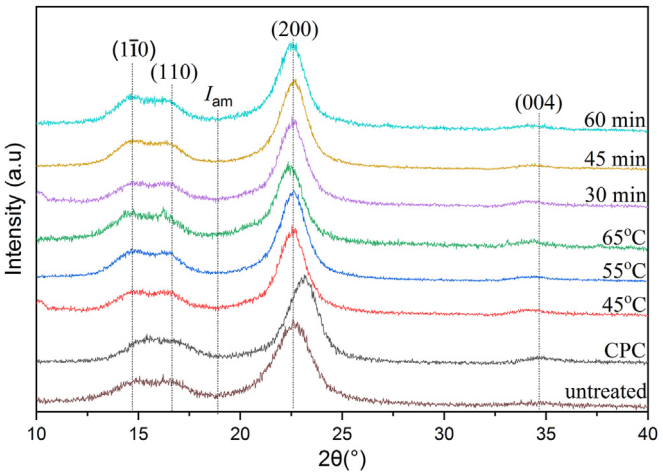

Figure 4. XRD patterns of untreated ramie fibers, CPC, and CNCs under different hydrolysis temperature and duration.

acid. All samples showed similar vibration bands, namely at 3400, 2900, 1635, 1427, 1373, 1056, and 894 cm^{-1}. The peaks at 3400 and 1635 cm^{-1} were related to the stretching and bending vibrations of the OH groups of cellulose [52, 53], respectively. The peak at 2900 cm^{-1} was attributed to the C–H stretching [54]. The peaks at 1427 cm^{-1} and 1373 cm^{-1} reflected the symmetric bending of CH_2 and the bending vibrations of the C–H and C–O groups of the aromatic rings in polysaccharides, respectively [55]. The peak at 1056 cm^{-1} was attributed to the C–O–C pyranose ring (anti-symmetric in phase ring) stretching vibration whereas the peak at 894 cm^{-1} related to C–H rock vibration of cellulose (anomeric vibration, specific for β-glucosies) [56]. The untreated ramie fibers showed a distinct band appearance compared to others where the peak at 1735 cm^{-1} appeared. The peak at 1735 cm^{-1} corresponded to carboxyl groups in the acids and esters of acetic, p-coumatic, ferulic, and uronic acids, which were the primary components of extractives and hemicellulose [54, 57, 58]. The absence of a peak at 1735 cm^{-1} in the spectra of CPC and CNCs indicated the elimination of hemicellulose and lignin during chemical purification and hydrolysis [14, 23]. Moreover, the small shoulder at 811 cm^{-1} was only observed in the CNCs representing C–O–S group vibration owing to the establishment of sulfate esters on the CNCs surface during hydrolysis [19,59]. There were no significant changes in the FT-IR spectra of the gained CNCs after sulfuric acid hydrolysis under different both hydrolysis temperature and time. It means that both hydrolysis temperature and time did not change the structure of cellulose. Moreover, the intensity of CNCs samples was higher compared to that of both untreated ramie fibers and CPC. The increased intensity might be related to the increased crystallinity of the fiber after chemical purification and hydrolysis of sulfuric acid [60].

3.2. X-ray diffraction (XRD)

The XRD patterns of untreated ramie fibers, CPC, and CNCs prepared under different both hydrolysis temperature and time are demonstrated in Figure 4. All samples displayed peaks at $2\theta = 15$, 16, 22, and 34° in accordance with the (1$\bar{1}$0), (110), (200), and (004) crystal planes, respectively, which represented the characteristic of cellulose Iβ structure [61]. These results showed that the structure characteristics of cellulose I did not changed by purification and sulfuric acid hydrolysis. The crystallinity index of CNCs at different hydrolysis conditions was determined using Segal equation (Eq.1) and their results were presented in Table 1. As for control, the crystallinity index of untreated ramie fibers and CPC were also determined and it was found that the crystallinity index of untreated ramie fibers and CPS were 79.75 and 86.68, respectively. This indicated that the chemical purification increased the crystallinity owing to the dissolving of hemicellulose and lignin [58, 62]. The crystallinity index of CNCs prepared at various temperatures of 45, 55, and 65 °C was 90.77, 87.99, and 80.32%, respectively. This suggested that the crystallinity index of CNCs prepared with hydrolysis temperatures of 45 and 55 °C was higher compared to that of both untreated ramie fibers and CPC. The removal of amorphous components due to sulfuric hydrolysis and structural changes in organization and alignment to produce highly ordered crystal bundles might be responsible for the increased crystallinity index of CNCs [15,63]. However, the crystallinity index of CNCs hydrolyzed at a temperature above 45 °C was reduced. This was related to the fact that at the higher temperature, acid hydrolysis removed amorphous components and also some parts of crystalline accelerating the hydrolytic cleavage of the glycosidic bonds and finally resulted in the decreased crystallinity [64]. Furthermore, the impact of hydrolysis time on the crystallinity index is presented in Table 1. The crystallinity index of CNCs made at various hydrolysis times of 30, 45, and 60 min was 90.77, 87.55, and 83.52%, respectively. This indicated that the crystallinity index reduced as the reaction time increased. This trend is similar to that of increasing the hydrolysis temperature (Table 1). At the reaction time more than 30 min, part of the cellulose crystalline domains of CNCs was removed due to corrosion by sulfuric acid and then resulted in the reduced crystallinity [65, 66]. These findings were also in line with those found by other researchers [64, 65]. Kargarzadeh et al. [65] demonstrated that the optimal reaction time was achieved in 40 min at 45 °C with 65% sulfuric acid on the production of CNC from kenaf bast fibers. Similar observations were demonstrated by Al-Dulaimi and Wanrosli [64] where the optimum hydrolysis time was achieved in 80 min by 58% sulfuric acid concentration on the extraction CNCs from oil palm empty fruit bunches. It is interesting to be concluded that both temperature and time of hydrolysis influenced the crystallinity of CNCs and the optimum hydrolysis conditions were achieved under hydrolysis conditions, namely at 45 °C for 30 min with 58% sulfuric acid concentration. The highest crystallinity index obtained in this study was 90.77% and this was a slight higher than that demonstrated by Habibi et al. [28]. CNC with 88% crystallinity index was prepared by Habibi et al. [28]. The slight difference was probably due to the slight difference in sulfuric acid concentration where Habibi et al. [28] used 65% H_2SO_4 solution in the hydrolysis process. The obtained crystallinity index was much higher compared to that declared by Syafri et al. [29] producing cellulose nanofibers from the ramie fibers with 73.65% crystallinity index. This difference was associated with the different methods used where Syafri et al. [29] used mixed chemical-ultrasonic method.

Table 1. Crystallinity index and crystallite size of CNCs produced under different hydrolysis conditions.

Temperature (°C)	Reaction time (min)	Sulfuric acid concentration (%)	Crystallinity (%)	Crystallite size (nm)
45	30	58	90.77	5.33
55	30	58	87.99	4.95
65	30	58	80.32	4.73
45	45	58	87.55	5.22
45	60	58	83.52	4.62

The crystallite size of CNCs made at various hydrolysis conditions was computed according to the Scherrer equation (Eq. 2) and the results were summarized in Table 1. The crystallite size of untreated ramie fibers and CPC was also determined as for comparison and their results were 3.74 and 4.75, respectively. This indicated that the chemical purification increased the crystallite size of CPC. The increase in CPC crystallite size might be believed to be mainly owing to the tightening of the crystal size distribution by chemical purification [15]. From Table 1, it was also found that the crystallite size of CNCs made at various temperatures of 45, 55, and 65 °C was 5.33, 4.95, and 4.73 nm, respectively. This exhibited that the crystallite size of CNCs reduced by increasing hydrolysis temperature. This trend was similar to the results of the crystallite size of CNCs by increasing reaction time (Table 1). The crystallite size of CNCs was reduced by increasing reaction time. This trend is similar to the crystallinity index. The decrease in the crystallite size of CNCs with increasing both temperature and reaction time during hydrolysis was associated with the stronger hydrolysis at both higher temperature and reaction time that eliminated the amorphous components and even portions of the crystalline component producing the reduced crystallite sizes [63].

3.3. Transmission electron microscopy

Figure 5 displays the TEM images of obtained CNCs produced with 58% sulfuric acid under different temperatures and durations of hydrolysis. It can be seen that all CNCs had a needle-like shape with a nanoscale dimension. Figure 5a displays the TEM image of CNC produced under hydrolysis by 58% sulfuric acid solution at 45 °C for 30 min whereas Figure 5b presents the TEM image of CNC produced under 58% sulfuric acid solution at 65 °C for 30 min. The TEM image of CNC made under hydrolysis by 58% sulfuric acid solution at 45 °C for 60 min is displayed in Figure 5c. Furthermore, the diameter and length of CNCs particles were analyzed by ImageJ taken from TEM images (Figure 5). Figure 6a-b exhibits the distribution of diameter and length of CNC made under hydrolysis condition at 45 °C for 30 min with 58% sulfuric acid) and it was found average 6.67 nm in diameter and 145.61 nm in length. This result was no significant difference with the result obtained by Habibi et al. [28] which produced CNCs with average 6.5 nm in diameter and average 185 nm in length. The diameter and length distributions of CNC prepared under hydrolysis by 58% sulfuric acid at 65 °C for 30 min are

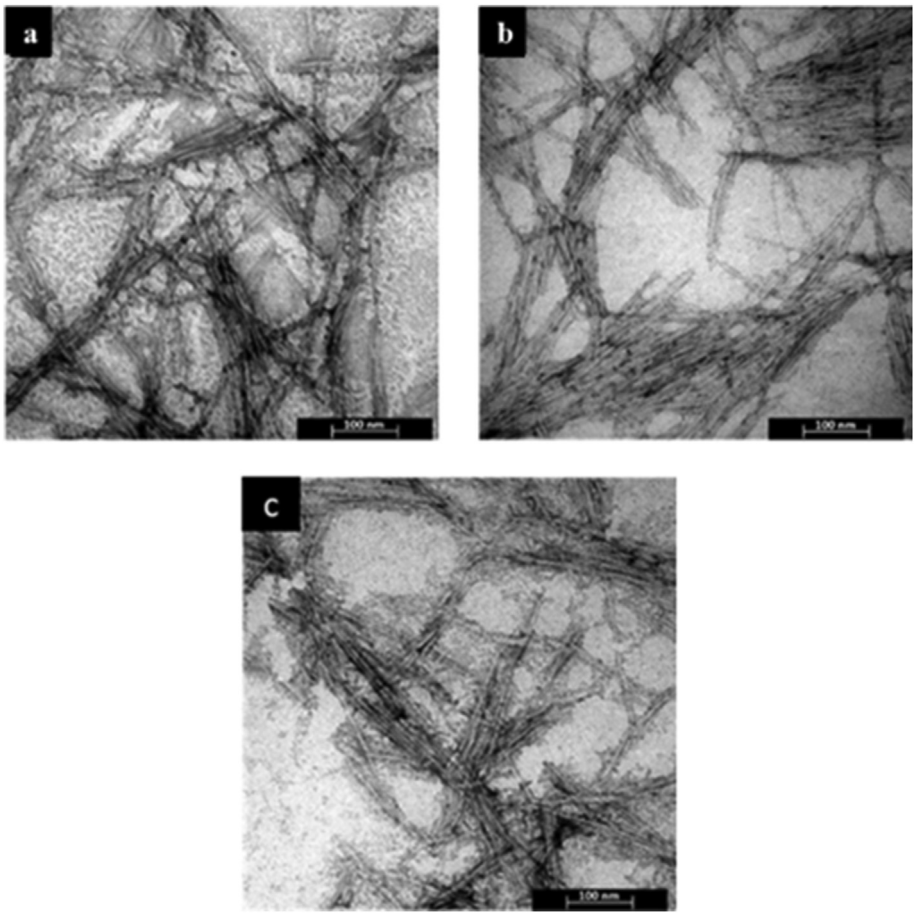

Figure 5. TEM images of obtained CNCs under different hydrolysis conditions with 58 wt% sulfuric acid at: (a) 45 °C for 30 min (b) 65 °C for 30 min, and (c) 45 °C for 60 min.

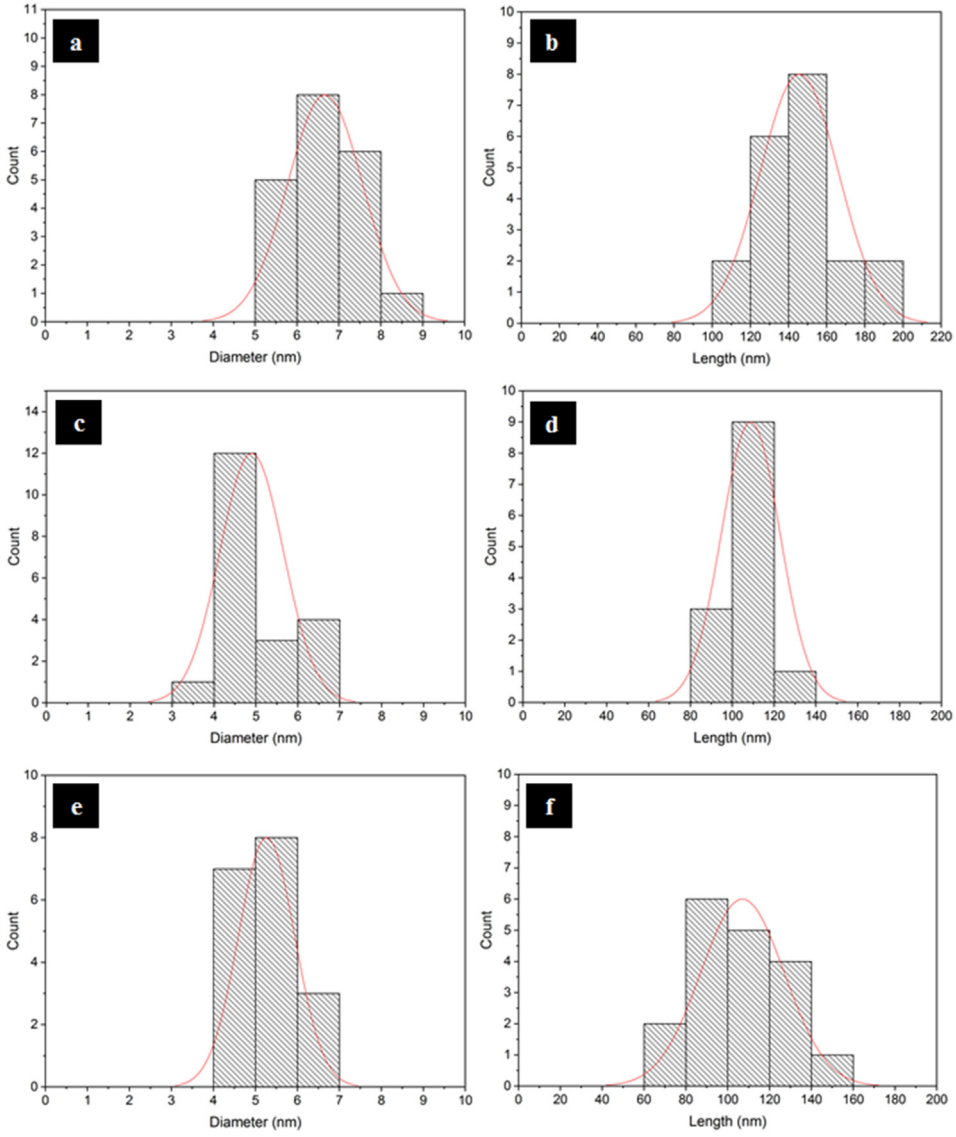

Figure 6. Diameter and length distribution of obtained CNCs under hydrolysis with 58 wt% sulfuric acid at: (a, b) 45 °C for 30 min (c, d) 65 °C for 30 min, and (e, f) 45 °C for 60 min.

shown in Figure 6c-d. The average diameter and length of the CNC were 4.9 nm and 108.78 nm, respectively. This indicated that by increasing hydrolysis temperature the diameter and length were decreased drastically. At higher hydrolysis temperature (above 45 °C), hydrolysis eliminated the amorphous domains and some parts of the crystalline domains, which then led to the reduced diameter and length of CNCs [64]. Figure 6e-f displays the classification of diameter and length of CNC made at 45 °C for 60 min by 58% sulfuric acid. The average diameter and

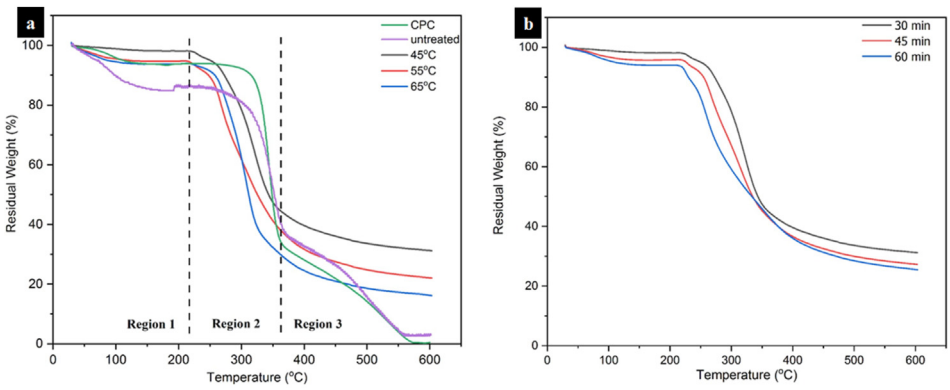

Figure 7. TGA curves of untreated ramie fibers, CPC, and obtained CNCs under hydrolysis with different (a) temperature and (b) duration.

Table 2. Initial temperature (Ti), maximum degradation temperature (T_{max}) and char yield ($W_{residue}$) for untreated ramie fibers, CPC, and CNCs at various hydrolysis conditions.

Sample	[a]T_i (°C)	[b]T_{10} (°C)	T_{max} (°C)	$W_{residue}$ (%)
Untreated ramie fibers	226	99	346	2,9
CPC	271	317	346	0,5
CNC 45 °C, 30 min	220	270	320	31
CNC 55 °C, 30 min	215	247	274	22
CNC 65 °C, 30 min	218	253	304	16
CNC 45 °C, 45 min	217	252	276	27
CNC 55 °C, 60 min	211	228	263	25

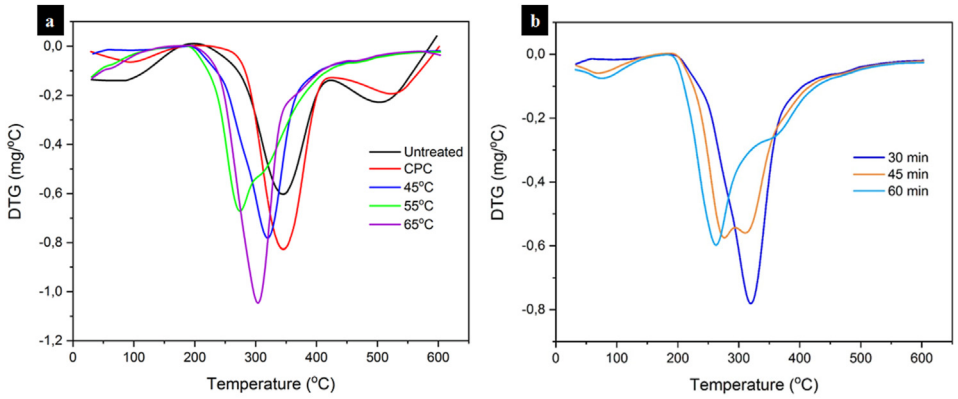

Figure 8. DTG curves of untreated ramie fibers, CPC, and obtained CNCs under hydrolysis with different (a) temperature and (b) duration.

length of the gained CNC were 5.26 nm and 107.02 nm, respectively. Compared to the CNC prepared under at 45 °C for 30 min, the CNC hydrolyzed for 60 min had a smaller average diameter and length. This indicated that the smaller dimension of CNCs was found with increasing reaction time. A similar observation was shown by the hydrolysis temperature effect as discussed earlier.

3.4. Thermogravimetry analysis (TGA)

Figure 7 shows the thermogravimetry (TG) curve from the untreated ramie fiber, CPC, and CNCs, and their results were displayed in Table 2. Figure 7a exhibits the TG curves of CNCs prepared under hydrolysis with different temperatures whereas Figure 7b displays the TG curves of CNCs prepared under hydrolysis with different reaction times. From Figure 7, all samples depict similar behavior with three regions of thermal degradation. Region I was 30–220 °C that was particularly attributed to the vaporization of moisture absorbed by all samples with a slight mass loss [67]. From Figures 7a and 7b, it can be seen that CNC prepared under hydrolysis at 45 °C for 30 min exhibited the lowest water weight loss among all samples. This was associated with the highest crystalline content of the CNC. This is consistent with the XRD analysis as discussed earlier. Furthermore, all samples exhibited the main stage of thermal degradation at a temperature range of 220–360 °C (Region II). This region showed the highest thermal degradation among all samples and cellulose experienced stronger depolymerization to produce volatiles including carbon monoxide, methane, and carbon dioxide [68]. Region III was 360–600 °C, which particularly demonstrated the further breakdown of thermal degradation intermediates, like levoglucosan and coke to produce volatile materials such as hydrogen, ethylene, ethane, and tar [69].

From Table 2, it can be found that the initial temperatures (T_i) at the main weight loss of the untreated ramie fibers, CPC, and CNCs were 226, 271, and 211–220 °C, respectively. The initial decomposition temperature of CPC was higher compared to that of untreated ramie fibers. This was related to the release of some hemicelluloses with lower thermal stability during the chemical purification, causing thermal stability to drop [70, 71]. Furthermore, the initial temperatures at the main degradation of CNCs hydrolyzed with 58% sulfuric acid concentration for 30 min with different temperatures of 45, 55, and 65 °C were 220, 215, and 218 °C, respectively. This suggested that thermal stability was reduced with increasing hydrolysis temperature. This was ascribed to more dissolution of crystalline regions of cellulose during hydrolysis at the higher temperatures (more than 45 °C) resulting in reduced crystallinity and then resulting in decreased thermal resistance. The onset degradation temperature of CNCs made at various hydrolysis times of 30, 45, and 60 min was 220, 217, and 211 °C, respectively. A similar effect was also exhibited by the hydrolysis time where the initial temperature at the main degradation of CNCs was also reduced with an increase of hydrolysis time. The T_i values of all CNCs were lower compared to those of untreated ramie fibers and CPC. This indicated that all CNCs displayed lower thermal stability than the untreated ramie fibers and CPC. The lower thermal resistance of CNCs was related to the existence of sulfate groups on the CNCs surface that catalyzed degradation [72]. From Table 2, it can also be observed that the thermal resistance of CNC was found to decrease with the increase of the hydrolysis time. This was due to the longer interaction between cellulose and sulfuric acid under hydrolysis resulted in more negatively charged sulfate groups on the CNCs surface resulting in decreased thermal resistance [73, 74]. It was concluded that both temperature and hydrolysis time have the same effect in reducing thermal stability. Similar findings were declared by Kargarzadeh et al. [65], Li et al. [75], and Haafiz et al. [76] who concluded that the addition of sulfate groups on the CNCs surface decreased the thermal resistance due to dehydration reaction.

Furthermore, changes in thermal stability are also observed at the 10% weight loss temperature (T_{10}) as shown in Table 2. The T_{10} of the untreated ramie fiber was lower than the CPC and all CNCs samples. The lower T_{10} of the untreated ramie fibers was caused by the high moisture content on the raw fibers owing to the existence of hemicellulose. The

dissolution of hemicellulose after purification increased to 317 °C for the CPC sample. However, the T_{10} of all CNCs samples was lower compared to that of the CPC caused by the addition of sulfate groups. The highest value in T_{10} of the CNCs samples was achieved for CNC hydrolyzed at 45 °C for 30 min. The T_{10} was then decreased as the increase in temperature and duration. This was ascribed to the removal of some parts of crystalline during hydrolysis thereby reducing both crystallinity index and crystallite size as discussed in the XRD test results. According to Haafiz et al. [76], the harsher condition of hydrolysis can lead to the dissolution of the crystalline domain and result in smaller crystallite sizes making it more susceptible to elevated temperature.

The decomposition peak temperature (T_{max}) for all samples can be observed in the DTG curves (Figure 8) and these values are summarized in Table 2. The major decomposition peaks of untreated ramie fibers and CPC occurred at a similar temperature of 346 °C and it was higher than that of CNCs. The higher thermal resistance was probably associated with the higher lignin content in both untreated raw fibers and CPC. Furthermore, lignin acted as a filler and linked to polysaccharides such as cellulose by covalent bonds, leading to the CNCs internal structure denser, which enhanced the thermal stability [77]. On the other hand, CNCs prepared under different temperatures of 45, 55, and 65 °C exhibited major degradation peaks at 320, 274, and 304 °C, respectively. Compared to both untreated ramie fibers and CPC, CNCs showed lower thermal stability. Furthermore, the major degradation peaks of CNCs made at various hydrolysis times of 30, 45, and 60 min were 320, 276, and 263 °C, respectively. This suggested that the maximum decomposition temperature of CNCs reduced by increasing the reaction time of hydrolysis. Both temperature and reaction time gave a similar effect in reducing the T_{max} of CNCs. This was ascribed to the smaller size CNCs with increasing both temperature and hydrolysis time as previously described in TEM images. Smaller CNC particles had a large surface area which caused an increase in heat transfer rate and finally reduced T_{max} as both temperature and hydrolysis time increased [78]. In addition, the thermal resistance of smaller size CNCs was lower than that of larger ones because smaller size CNCs had a much larger specific surface area and were more possible to expose during heating. This led to the accelerated pyrolysis rate and finally resulting in reduced thermal stability [79, 80]. From the dimension measurements taken from TEM images as discussed earlier, the smaller diameter and length were found by increasing both temperature and reaction time of hydrolysis. Moreover, with increasing hydrolysis time, the number of ester sulfate groups on the CNCs surfaces induced by hydrolysis increased, and then it led to the lower thermal stability. This is in good agreement between the TGA results and TEM observations. Furthermore, the residual weight of all CNCs at around 600 °C was much higher than that of both untreated ramie fibers and CPC. This was ascribed to the attached sulfate groups on the CNCs during hydrolysis as flame retardants [75, 77]. From Table 2, it can also be seen that there were differences in final residue among all CNCs. This was probably attributed to differences in the chemical structure and crystallinity of CNCs [81]. The final residues of CNCs decreased with increasing both the temperature and time of hydrolysis due to the decreased crystallinity index. This is in line with the results of the crystallinity index by increasing both temperature and time for hydrolysis (Table 1). These results were found to be similar to the results obtained by other researchers [62,81]. The final residual weight at 600 °C is strongly influenced by the cellulose resources and hydrolysis parameters for the isolation of CNCs [81].

4. Conclusion

CNCs were produced from ramie fibers via chemical pretreatments accompanied by sulfuric acid hydrolysis. Both chemical purification and sulfuric acid hydrolysis unchanged the chemical structure of cellulose I as indicated by FT-IR and XRD findings. The optimal hydrolysis was achieved at 45 °C for 30 min with 58% sulfuric acid that producing rod-like CNC particles with high crystallinity index (90.77%), the crystallite size (5.81 nm), average diameter (6.67 nm), and average length (145.61 nm). Both temperature and reaction time played an important role in the crystallinity, crystallite size, dimensions, and thermal resistance of CNCs. The crystallinity, crystallite size, dimensions, and thermal resitance of CNCs were attained to be reduce with the increase of both temperature and reaction time of hydrolysis. The results indicated that the obtained CNCs with high crystallinity (90.77%) had high potential as reinforcing materials for nanocomposites.

Declarations

Author contribution statement

Kusmono: Conceived and designed the experiments; Contributed reagents, materials, analysis tools or data; Wrote the paper.

R. Faiz Listyanda: Performed the experiments.

Muhammad Waziz Wildan: Analyzed and interpreted the data.

Mochammad Noer Ilman: Contributed reagents, materials, analysis tools or data.

Funding statement

This work was supported by Universitas Gadjah Mada and Ministry of Research, Technology and Higher Education, Indonesia Government under Hibah Penelitian Dasar Unggulan Perguruan Tinggi (110/UN1/DITLIT/DITLIT/LIT/2018 and 2645/UN1.DITLIT/DIT-LIT/LT/2019).

Data availability statement

Data included in article/supplementary material/referenced in article.

Declaration of interests statement

The authors declare no conflict of interest.

Additional information

No additional information is available for this paper.

References

[1] M.A.S.A. Samir, F. Alloin, M. Paillet, A. Dufresne, Tangling effect in fibrillated cellulose reinforced nanocomposites, Macromolecules 37 (2004) 4313–4316.

[2] D. Klemm, F. Kramer, S. Moritz, T. Lindström, M. Ankerfors, D. Gray, A. Dorris, Nanocelluloses: a New family of nature-based materials, Angew. Chem. Int. 50 (2011) 5438–5466.

[3] A.Y. Melikoğlu, S.E. Bilek, S. Cesur, Optimum alkaline treatment parameters for the extraction of cellulose and production of cellulose nanocrystals from apple pomace, Carbohydr. Polym. 2015 (2019) 330–337.

[4] H. Du, W. Liu, M. Zhang, C. Si, X. Zhang, B. Li, Cellulose nanocrystals and cellulose nanofibrils based hydrogels for biomedical applications, Carbohydr. Polym. 209 (2019) 130–144.

[5] L. Brinchi, F. Cotana, E. Fortunati, J.M. Kenny, Production of nanocrystalline cellulose from lignocellulosic biomass : Technology and applications, Carbohydr. Polym. 94 (2013) 154–169.

[6] E. Lam, K.B. Male, J.H. Chong, A.C.W. Leung, J.H. T Luong, Applications of functionalized and nanoparticle-modified nanocrystalline cellulose, Trends Biotechnol. 30 (5) (2012) 283–290.

[7] A. Dufresne, J.-Y. Cavaillé, W. Helbert, Thermoplastic nanocomposites filled with wheat straw cellulose whiskers. Part II: effect of processing and modeling, Polym. Compos. 18 (2) (1997) 198–210.

[8] N.L. Garcia de Rodriguez, W. Thielemans, A. Dufresne, Sisal cellulose whiskers reinforced polyvinyl acetate nanocomposites, Cellulose 13 (3) (2006) 261–270.

[9] B.M. Cherian, A.L. Leão, S.F. de Souza, S. Thomas, L.A. Pothan, M. Kottaisamy, Isolation of nanocellulose from pineapple leaf fibres by steam explosion, Carbohydr. Polym. 81 (3) (2010) 720–725.

[10] M.F. Rosa, E.S. Medeiros, J.A. Malmonge, K.S. Gregorski, D.F. Wood, L.H.C. Mattoso, S.H. Imam, Cellulose nanowhiskers from coconut husk fibers: effect of preparation conditions on their thermal and morphological behavior, Carbohydr. Polym. 81 (1) (2010) 83–92.

[11] B. Deepa, E. Abraham, B.M. Cherian, A. Bismarck, J.J. Blaker, L.A. Pothan, M. Kottaisamy, Structure, morphology and thermal characteristics of banana nano fibers obtained by steam explosion, Bioresour. Technol. 102 (2) (2011) 1988–1997.
[12] E. de Morais Teixeira, T.J. Bondancia, K.B.R. Teodoro, A.C. Corrêa, J.M. Marconcini, L.H.C. Mattoso, Sugarcane bagasse whiskers: extraction and characterizations, Ind. Crop. Prod. 33 (63) (2011) 63–66.
[13] B.S.L. Brito, F.V. Pereira, J.-L. Putaux, B. Jean, Preparation, morphology and structure of cellulose nanocrystals from bamboo fibers, Cellulose 19 (5) (2012) 1527–1536.
[14] R.M. Sheltami, I. Abdullah, I. Ahmad, A. Dufresne, H. Kargarzadeh, Extraction of cellulose nanocrystals from mengkuang leaves (Pandanus tectorius), Carbohydr. Polym. 88 (2) (2012) 772–779.
[15] P. Lu, Y. Hsieh, Preparation and characterization of cellulose nanocrystals from rice straw, Carbohydr. Polym. 87 (1) (2012) 564–573.
[16] J.P.S. Morais, M.D.F. Rosa, M. de Souza Filho, M. desá, L.D. Nascimento, D.M. do Nascimento, A.R. Cassales, Extraction and characterization of nanocellulose structures from raw cotton linter, Carbohydr. Polym. 91 (1) (2013) 229–235.
[17] L.H. Zaini, M. Jonoobi, P.M. Tahir, S. Karimi, Isolation and characterization of cellulose whiskers from kenaf (Hibiscus cannabinus) bast fibers, J. Biomaterials Nanobiotechnol. 4 (1) (2013) 37–44.
[18] C.A. de Carvalho Mendes, N.M.S. Ferreira, C.R.G. Furtado, A.M.F. de Sousa, Isolation and characterization of nanocrystalline cellulose from corn husk, Mater. Lett. 1481 (2015) 26–29.
[19] L. Jasmani, S. Adnan, Preparation and characterization of nanocrystalline cellulose from Acacia mangium and its reinforcement potential, Carbohydr. Polym. 161 (2017) 166–171.
[20] R. Dungani, A.F. Owolabi, C.K. Saurabh, H.P.S.A. Khalil, P.M. Tahir, C.I.I.C.M. Hazwan, K.A. Ajijolakewu, M.M. Masri, E. Rosamah, P. Aditiawati, Preparation and fundamental characterization of cellulose nanocrystal from oil palm frond biomass, J. Polym. Environ. 25 (2017) 692–700.
[21] M. Fardioui, A. Stambouli, T. Gueddira, A. Dahrouch, A.E.K. Qaiss, R. Bouhfid, Extraction and characterization of nanocrystalline cellulose from Doum (Chamaerops humilis) Leaves: a potential reinforcing biomaterial, J. Polym. Environ. 24 (2016) 356–362.
[22] A.P. Travalini, E. Prestes, L.A. Pinheiro, I.M. Demiate, Extraction and characterization of nanocrystalline cellulose from cassava bagasse, J. Polym. Environ. 26 (2018) 789–797.
[23] R.A. Ilyas, S.M. Sapuan, M.R. Ishak, Isolation and characterization of nanocrystalline cellulose from sugar palm fibres (Arenga Pinnata), Carbohydr. Polym. 181 (2018) 1038–1051.
[24] X.Q. Chen, G.X. Pang, W.H. Shen, X. Tong, M.Y. Jia, Preparation and characterization of the ribbon-like cellulose nanocrystals by the cellulase enzymolysis of cotton pulp fibers, Carbohydr. Polym. 2071 (2019) 713–719.
[25] E. Galiwango, N.S. Abdel Rahman, A.H. Al-Marzouqi, M.M. Abu-Omar, A.A. Khaleel, Isolation and characterization of cellulose and α-cellulose from date palm biomass waste, Heliyon 5 (2019), e02937.
[26] Kusmono, M.W. Wildan, M.N. Ilman, A preliminary study of extraction and characterization of nanocrystalline cellulose (NCC) from ramie fiber, J. Mater. Proc. Char. 1 (2020) 42–46.
[27] Y. Habibi, A.L. Goffin, N. Schiltz, E. Duquesne, P. Dubois, A. Dufresne, Bionanocomposites based on poly(*3*-caprolactone)-grafted cellulose nanocrystals by ring-opening polymerization, J. Mater. Chem. 18 (2008) 5002–5010.
[28] Y. Habibi, I. Hoeger, S.S. Kelley, O.J. Rojas, Development of Langmuir-Schaeffer cellulose nanocrystal monolayers and their interfacial behaviors, Langmuir 26 (2) (2010) 990–1001.
[29] E. Syafri, A. Kasim, H. Abral, A. Asben, Cellulose nanofibers isolation and characterization from ramie using a chemical-ultrasonic treatment, J. Nat. Fibers 16 (8) (2019) 1–11.
[30] S.Y. Lee, S.J. Chun, I.A. Kang, J.Y. Park, Preparation of cellulose nanofibrils by high pressure homogenizer and cellulose-based composite films, J. Ind. Eng. Chem. 15 (2009) 50–55.
[31] S. Nie, C. Zhang, Q. Zhang, K. Zhang, Y. Zhang, P. Tao, S. Wang, Enzymatic and cold alkaline pretreatments of sugarcane bagasse pulp to produce cellulose nanofibrils using a mechanical method, Ind. Crop. Prod. 124 (2018) 435–441.
[32] T. Saito, M. Hirota, N. Tamura, S. Kimura, H. Fukuzumi, L. Heux, A. Isogai, Individualization of nano-sized plant cellulose fibrils by direct surface carboxylation using tempo catalyst under neutral conditions, Biomacromolecules 10 (2009) 1992–1996.
[33] H. Ma, B. Zhou, H.S. Li, Y.Q. Li, S.Y. Ou, Green composite films composed of cellulose nanocrystals and a cellulose matrix regenerated from functionalized ionic liquid solution, Carbohydr. Polym. 84 (2011) 383–389.
[34] S. Nie, K. Zhang, X. Lin, C. Zhang, D. Yan, H. Liang, S. Wang, Enzymatic pretreatment for the improvement of dispersion and film properties of cellulose nanofibrils, Carbohydr. Polym. 181 (2018) 1136–1142.
[35] M. Henriksson, G. Henriksson, L.A. Berglund, T. Lindström, An environmentally friendly method for enzyme-assisted preparation of microfibrillated cellulose (MFC) nanofibers, Eur. Polym. J. 43 (2007) 3434–3441.
[36] T. Kos, A. Anžlovar, M. Kunaver, M. Huskić, E. Žagar, Fast preparation of cellulose nanocrystals by microwave-assisted hydrolysis, Cellulose 21 (2014) 2579–2585.
[37] F. Beltramino, M.B. Roncero, A.L. Torres, T. Vidal, C. Valls, Optimization of sulfuric acid hydrolysis conditions for preparation of cellulose nanocrystals from enzymatically pretreated fibers, Cellulose 23 (2016) 1777–1789.
[38] A.C. Corrêa, E.M. de Teixeira, L.A. Pessan, L.H.C. Mattoso, Cellulose nanofibers from curaua fibers, Cellulose 17 (6) (2010) 1183–1192.
[39] A.A. Oun, J.W. Rhim, Effect of post-treatments and concentration of cotton linter cellulose nanocrystals on the properties of agar-based nanocomposite films, Carbohydr. Polym. 134 (2015) 20–29.
[40] F. Shen, W. Xiao, L. Lin, G. Yang, Y. Zhang, S. Deng, Enzymatic saccharification coupling with polyester recovery from cotton-based waste textiles by phosphoric acid pretreatment, Bioresour. Technol. 130 (2013) 248–255.
[41] Y.J. Tang, X.C. Shen, J.H. Zhang, D.L. Guo, F.G. Kong, N. Zhang, Extraction of cellulose nano-crystals from old corrugated container fiber using phosphoric acid and enzymatic hydrolysis followed by sonication, Carbohydr. Polym. 125 (2015) 360–366.
[42] B. Li, W. Xu, D. Kronlund, A. Määttänen, J. Liu, Jan-Henrik Smått, J. Peltonen, S. Willför, X. Mu, C. Xu, Cellulose nanocrystals prepared via formic acid hydrolysis followed by TEMPO-mediated oxidation, Carbohydr. Polym. 133 (2015) 605–612.
[43] H. Xie, Z. Zou, H. Du, X. Zhang, X. Wang, X. Yang, H. Wang, G. Li, L. Li, C. Si, Preparation of thermally stable and surface-functionalized cellulose nanocrystals via mixed H_2SO_4/Oxalic acid hydrolysis, Carbohydr. Polym. 223 (2019) 115116.
[44] H. Wang, H. Xie, H. Du, X. Wang, W. Liu, Y. Duan, X. Zhang, L. Sun, X. Zhang, C. Si, Highly efficient preparation of functional and thermostable cellulose nanocrystals via H_2SO_4 intensified acetic acid hydrolysis, Carbohydr. Polym. 239 (2020) 116233.
[45] X. Yang, H. Xie, H. Du, X. Zhang, Z. Zou, Y. Zou, W. Liu, H. Lan, X. Zhang, C. Si, Facile extraction of thermally stable and dispersible cellulose nanocrystals with high yield via a green and recyclable $FeCl_3$-Catalyzed Deep Eutectic Solvent System, ACS Sustain. Chem. Eng. 7 (7) (2019) 7200–7208.
[46] H. Du, M. Parit, M. Wu, X. Che, Y. Wang, M. Zhang, R. Wang, X. Zhang, Z. Jiang, B. Li, Sustainable valorization of paper mill sludge into cellulose nanofibrils and cellulose nanopaper, J. Hazard Mater. 400 (2020) 123106.
[47] K. Abe, Y. Yano, Comparison of the characteristics of cellulose microfibril aggregates of wood, rice straw and potato tuber, Cellulose 16 (6) (2009) 1017–1023.
[48] A. Kumar, Y. Singh Negi, V. Choudhary, N.K. Bhardwaj, Characterization of cellulose nanocrystals produced by acid-hydrolysis from sugarcane bagasse as agro-waste, J. Mat. Phys. Chem. 2 (1) (2014) 1–8.
[49] R.F. Listyanda, Kusmono, M.W. Wildan, M.N. Ilman, Extraction and characterization of nanocrystalline cellulose (NCC) from ramie fiber by sulphuric acid hydrolysis, AIP Conf. Proc. 2217 (2020), 030069.
[50] L. Segal, J.J. Creely, A.E. Martin, C.M. Conrad, An empirical method for estimating the degree of crystallinity of native cellulose using the X-Ray Diffractometer, Textil. Res. J. 29 (1959) 786–794.
[51] M.L. Normand, R. Moriana, M. Ek, Isolation and characterization of cellulose nanocrystals from spruce bark in a biorefinery perspective, Carbohydr. Polym. 111 (2014) 979–987.
[52] Y.J. Tang, S.J. Yang, N. Zhang, J.H. Zhang, Preparation and characterization of nanocrystalline cellulose via low-intensity ultrasonic-assisted sulfuric acid hydrolysis, Cellulose 21 (2014) 335–346.
[53] F.A. Ngwabebhoh, A. Erdem, U. Yildiz, A design optimization study on synthesized nanocrystalline cellulose, evaluation, and surface modification as a potential biomaterial for prospective biomedical applications, Int. J. Biol. Macromol. 114 (2018) 536–546.
[54] M. Sain, S. Panthapulakkal, Bioprocess preparation of wheat straw fibers and their characterization, Ind. Crop. Prod. 23 (2006) 1–8.
[55] M. Jonoobi, J. Harun, A. Shakeri, M. Misra, K. Oksman, Chemical composition, crystallinity, and thermal degradation of bleached and unbleached kenaf bast (Hibiscus cannabinus) pulp and nanofibers, BioResources 4 (2) (2009) 626–639.
[56] W. Lei, C. Fang, X. Zhou, Q. Yin, S. Pan, R. Yang, D. Liu, Y. Ouyang, Cellulose nanocrystals obtained from office waste paper and their potential application in PET packing materials, Carbohydr. Polym. 181 (2018) 376–385.
[57] X.F. Sun, R. Sun, P. Fowler, M.S. Baird, Extraction and characterization of original lignin and hemicelluloses from wheat straw, J. Agric. Food Chem. 53 (2005) 860–870.
[58] A. Alemdar, M. Sain, Isolation and characterization of nanofibers from agricultural residues–Wheat straw and soy hulls, Bioresour. Technol. 99 (6) (2008) 1664–1671.
[59] J. Han, C. Zhou, Y. Wu, F. Liu, Q. Wu, Self-assembling behavior of cellulose nanoparticles during freeze-drying: effect of suspension concentration, particle size, crystal structure, and surface charge, Biomacromolecules 14 (5) (2013) 1529–1540.
[60] R.T. O'Connor, E.F. DuPré, D. Mitcham, Applications of infrared absorption spectroscopy to investigations of cotton and modified cottons: Part I: physical and crystalline modifications and oxidation, Textil. Res. J. 28 (5) (1958) 382–392.
[61] A.D. French, Idealized powder diffraction patterns for cellulose polymorphs, Cellulose 21 (2014) 885–896.
[62] W. Chen, H. Yu, Y. Liu, P. Chen, M. Zhang, Y. Hai, Individualization of cellulose nanofibers from wood using high-intensity ultrasonication combined with chemical pretreatments, Carbohydr. Polym. 83 (4) (2011) 1804–1811.
[63] M.A.S.A. Samir, F. Alloin, M. Paillet, A. Dufresne, Tangling effect in fibrillated cellulose reinforced nanocomposites, Macromolecules 37 (2004) 4313–4316.
[64] A.A. Al-Dulaimi, W.D. Wanrosli, Isolation and characterization of nanocrystalline cellulose from totally chlorine free oil palm empty fruit bunch pulp, J. Polym. Environ. 25 (2017) 192–202.
[65] H. Kargarzadeh, I. Ahmad, I. Abdullah, A. Dufresne, S.Y. Zainudin, R.M. Sheltami, Effects of hydrolysis conditions on the morphology, crystallinity, and thermal

stability of cellulose nanocrystals extracted from kenaf bast fibers, Cellulose 19 (2012) 855–866.
[66] L.K. Kian, M. Jawaid, H. Arif, Z. Karim, Isolation and characterization of nanocrystalline cellulose from roselle-derived microcrystalline cellulose, Int. J. Biol. Macromol. 114 (2018) 54–63.
[67] Y. Jiang, J. Zhou, Q. Zhang, G. Zhao, L. Heng, D. Chen, D. Liu, Preparation of cellulose nanocrystals from Humulus japonicus stem and the influence of high temperature pretreatment, Carbohydr. Polym. 164 (2017) 284–293.
[68] A. Isaac, J. de Paula, C.M. Viana, A.B. Henriques, A. Malachias, L.A. Montoro, From nano- to micrometer scale: the role of microwave-assisted acid and alkali pretreatments in the sugarcane biomass structure, Biotechnol. Biofuels 11 (73) (2018) 1–11.
[69] H. Yang, R. Yan, H. Chen, H.L. Dong, C. Zheng, Characteristics of hemicellulose, cellulose and lignin pyrolysis, Fuel 86 (2007) 1781–1788.
[70] A. Sonia, K.P. Dasan, Chemical, morphology and thermal evaluation of cellulose microfibers obtained from Hibiscus sabdariffa, Carbohydr. Polym. 92 (1) (2013) 668–674.
[71] P. Tao, Zhengmei Wu, Chuyue Xing, Q. Zhang, Z. Wei, S. Nie, Effect of enzymatic treatment on the thermal stability of cellulose nanofibrils, Cellulose 26 (2019) 7717–7725.
[72] M. Roman, W.T. Winter, Effect of sulfate groups from sulfuric acid hydrolysis on the thermal degradation behavior of bacterial cellulose, Biomacromolecules 5 (5) (2004) 1671–1677.
[73] N. Wang, E. Ding, R. Cheng, Thermal degradation behaviors of spherical nanocrystalline cellulose with sulfate groups, Polymer 48 (2007) 3486–3493.
[74] Y. Chen, C. Liu, P.R. Chang, X. Cao, D.P. Anderson, Bionanocomposites based on pea starch and cellulose nanowhiskers hydrolyzed from pea hull fibre: effect hydrolysis time, Carbohydr. Polym. 76 (2009) 607–615.
[75] R. Li, J. Fei, Y. Cai, Y. Li, J. Feng, J. Yao, Cellulose whiskers extracted from mulberry: a novel biomass production, Carbohydr. Polym. 76 (1) (2009) 94–99.
[76] M.K.M. Haafiz, A. Hassan, Z. Zakaria, I.M. Inuwa, Isolation and characterization of cellulose nanowhiskers from oil palm biomass microcrystalline cellulose, Carbohydr. Polym. 103 (2014) 119–125.
[77] N. Zhang, P. Tao, Y. Lu, S. Nie, Effect of lignin on the thermal stability of cellulose nanofibrils produced from bagasse pulp, Cellulose 26 (2019) 7823–7835.
[78] F. Jiang, Y. Hsieh, Chemically and mechanically isolated nanocellulose and their self-assembled structures, Carbohydr. Polym. 95 (2013) 32–40.
[79] N. Quiévy, N. Jacquet, M. Sclavons, C. Deroanne, M. Paquot, J. Devaux, Influence of homogenization and drying on the thermal stability of microfibrillated cellulose, Polym. Degrad. Stabil. 95 (2010) 306–314.
[80] K. Zhang, Y. Zhang, D. Yan, C. Zhang, S. Nie, Enzyme-assisted mechanical production of cellulose nanofibrils: thermal stability, Cellulose 25 (2018) 5049–5061.
[81] A.A. Oun, J.W. Rhim, Isolation of cellulose nanocrystals from grain straws and their use for the preparation of carboxymethyl cellulose-based nanocomposite films, Carbohydr. Polym. 150 (2016) 187–200.